

## Research Paper

# Injectable polypeptide hydrogel-based co-delivery of vaccine and immune checkpoint inhibitors improves tumor immunotherapy

Huijuan Song<sup>1</sup>, Pengxiang Yang<sup>1</sup>, Pingsheng Huang<sup>1</sup>✉, Chuangnian Zhang<sup>1</sup>, Deling Kong<sup>1, 2, 3</sup>✉, Weiwei Wang<sup>1, 4</sup>✉

1. Tianjin Key Laboratory of Biomaterial Research, Institute of Biomedical Engineering, Chinese Academy of Medical Sciences and Peking Union Medical College, Tianjin 300192, China
2. State Key Laboratory of Medicinal Chemical Biology, the Key Laboratory of Bioactive Materials, Ministry of education, College of Life Sciences, Nankai University, Tianjin 300071, China
3. Jiangsu Center for the Collaboration and Innovation of Cancer Biotherapy, Cancer Institute, Xuzhou Medical University, Xuzhou 221004, Jiangsu, China
4. State Key Laboratory of Molecular Engineering of Polymers (Fudan University), Shanghai 200433, China

✉ Corresponding authors: Dr. Wang, E-mail: [wwwangtj@163.com](mailto:wwwangtj@163.com); Dr. Huang, E-mail: [sheng1989.2008@163.com](mailto:sheng1989.2008@163.com); Prof. Dr. Kong, E-mail: [kongdeling@nankai.edu.cn](mailto:kongdeling@nankai.edu.cn)

© Ivyspring International Publisher. This is an open access article distributed under the terms of the Creative Commons Attribution (CC BY-NC) license (<https://creativecommons.org/licenses/by-nc/4.0/>). See <http://ivyspring.com/terms> for full terms and conditions.

Received: 2018.10.11; Accepted: 2019.02.24; Published: 2019.04.12

## Abstract

Immunotherapy, an attractive option for cancer treatment, necessitates the direct stimulation of immune cells *in vivo* and the simultaneous effective inhibition of immunosuppressive tumor microenvironments.

**Methods:** In the present study, we developed an injectable PEG-*b*-poly(L-alanine) hydrogel for co-delivery of a tumor vaccine and dual immune checkpoint inhibitors to increase tumor immunotherapy efficacy. Tumor cell lysates, granulocyte-macrophage colony stimulating factor (GM-CSF), and immune checkpoint inhibitors (anti-CTLA-4/PD-1 antibody) were readily encapsulated in the porous hydrogel during the spontaneous self-assembly of polypeptide in aqueous solution.

**Results:** Sustained release of tumor antigens and GM-CSF persistently recruited and activated dendritic cells (DCs) and induced a strong T-cell response *in vivo*, which was further enhanced by the immune checkpoint therapy. The hydrogel vaccine also upregulated the production of IgG and the secretion of cytokines including IFN- $\gamma$ , IL-4, and TNF- $\alpha$ . Importantly, the hydrogel-based combination therapy had superior immunotherapy effects against melanoma and 4T-1 tumor in comparison with the vaccine alone or in addition with a single immune checkpoint blockade. In studying the underlying mechanism, we found that the hydrogel-based combinatorial immunotherapy not only significantly increased the activated effector CD8<sup>+</sup> T cells within the spleens and tumors of vaccinated mice, but also reduced the ratio of Tregs.

**Conclusion:** Our findings indicate that the polypeptide hydrogel can be used as an effective sustained delivery platform for vaccines and immune checkpoint inhibitors, providing an advanced combinatorial immunotherapy approach for cancer treatment.

Key words: Cancer immunotherapy, vaccine, immune checkpoint blockade, hydrogel, drug delivery.

## Introduction

Cancer immunotherapy is a promising strategy that activates the body's immune system to fight tumors. Recent decades have witnessed numerous advances in this field. Today, several powerful approaches including cancer vaccines [1-3], immune checkpoint blockade [4-6], and adoptive cell transfer [7-9], have achieved significant increases in antitumor

immunity and patient survival in clinical trials. These approaches have their own strengths and limitations, but active immunization by cancer vaccines is considered a key tool for effective cancer immunotherapy, and holds great promise for personalized cancer treatment [10, 11]. Cancer vaccines aim to activate and amplify tumor-specific

T-cell immunity, allowing effector CD8<sup>+</sup> T cells to seek, capture and eradicate cancer cells. Diverse types of antigens including viral vectors, bacterial strains, recombinant proteins, whole tumor lysates, nucleic acids, and synthetic peptides have been used for rational vaccine design [3, 12-14]. Unfortunately, a few antigens such as tumor lysates, nucleic acids, proteins and peptides suffer low immunogenicity [15, 16], owing to their low efficiency, degradation, or to lower uptake by antigen-presenting cells (APCs), thus eliciting insufficient vaccine-specific T-cell responses on their own. Thus, cancer vaccines are usually used in combination with adjuvants or delivery systems [16-21] that can assist the activation of APCs such as dendritic cells (DCs), protect antigens from degradation, and improve their uptake by DCs, to prolong their duration *in vivo* and enhance their drainage to lymph nodes, whereby, they provoke a much stronger antigen-specific T-cell immune response. Whereas, tumor immunosuppression can downregulate the activation of T-cells, inhibit T-cell infiltration in tumors and thereby decrease cancer-specific cytotoxic T-cell numbers or even cause T-cell anergy or exhaustion [4, 22]. In this regard, immune checkpoint blockade using monoclonal antibodies or small molecule drugs against programmed cell death protein-1 (PD-1), indoleamine 2,3-dioxygenase (IDO), or cytotoxic T lymphocyte antigen-4 (CTLA-4) signaling pathways has shown promising clinical antitumor activity in melanoma [5, 6]. Nevertheless, this approach suffers from low objective response rate, systemic toxicity, and unavailability to a growing range of malignancy types such as pancreatic and colorectal cancer.

Recently, biomaterials-based immunomodulation has emerged as an innovative, versatile, and powerful approach to direct cancer-specific T-cell responses and immune checkpoint inhibition [17-19, 23-27]. In principle, engineered biomaterials including nanoparticles and microcapsules can encapsulate and deliver various immune-stimulatory cargoes such as antigens, cytokines and antibodies in a spatiotemporally controlled manner, either to facilitate antigen uptake by APCs, promote the stimulation of immune cells, to increase T-cell response, or remodel the tumorous microenvironment, to enhance immune checkpoint blockade [28-33]. For example, synthetic polymeric nanoparticles [34] and lipoprotein-mimicking nanodiscs [12] has been developed to generate strong antigen-specific cytotoxic T-cell responses and inhibit the growth of several types of tumors. Nanoparticle-based toll-like receptor (TLR) agonist delivery for macrophage polarization or DC activation can also enhance the efficiency of cancer

immunotherapy [35-37]. Macroscale drug delivery systems such as mesoporous silica micro-rod scaffolds, implants and injectable hydrogels also could enhance the immunogenicity of cancer vaccines [38-45], stimulate the activation of host dendritic cells (DCs) and T-cell response, and delay tumor growth. Likewise, various biomaterials have also shown great promise for enhancing immune checkpoint blockade [26, 46-48]. Biomaterials-based immunomodulation may be a key strategy to significantly improve the antitumor T-cell response either by increasing vaccine immunogenicity or by reducing tumor immunosuppression, and combining vaccines with the inhibition of tumoral immunosuppression may further improve immunotherapy efficiency, and is worthy of further study.

Herein, we developed a self-assembled mPEG-*b*-poly(L-alanine) hydrogel to encapsulate a tumor vaccine comprised of tumor cell lysates (TCLs) and granulocyte-macrophage colony-stimulating factor (GM-CSF), which has been identified as a potent stimulator for the recruitment, phenotype modulation and proliferation of DCs, and has undergone clinical testing as a vaccine adjuvant [49, 50]. These were combined with dual immune checkpoint inhibitors to synergistically modulate T-cell immunity and inhibit the tumor immunosuppression. The sustained presentation of the tumor vaccine is supposed to persistently recruit and activate DCs directly *in vivo*, which then primes the tumor-specific effector CD8<sup>+</sup>T-cell response. Meanwhile, extended release of inhibitors including anti-PD-1 and anti-CTLA-4 antibodies from the hydrogel enables the blockage of PD-1 and CTLA-4 pathways, reducing the production of regulatory T-cells (Tregs) in tumor. Collaboratively, such a hydrogel-based combinatorial immunotherapy is expected to significantly augment tumor-infiltrating CD8<sup>+</sup> T-cells, and consequently, increasing the efficiency of immunotherapy against B16F10 melanoma and 4T-1 tumors.

## Materials and methods

### Animals, cells, antibodies, and chemical reagents

C57BL/6 female mice (6-8 weeks old) were purchased from the Academy of Military Medical Sciences (Beijing, China). All of the animal procedures were performed in accordance with the rules established by the Center of Tianjin Animal Experiment Ethics Committee and Authority for Animal Protection (certification number: SYXK (Jin) 2011-0008). B16 cells were obtained from the American Type Culture Collection (ATCC, Manassas,

VA, USA) and cultured according to the manufacturer's guidelines. Fluorochrome-conjugated anti-mouse monoclonal antibodies specific for CD3e (clone 145-2C11), CD8a (clone 53-6.7), CD4 (clone GK1.5), CD86 (clone GL-1), CD40 (clone 3/23), and CD11c (clone N418) were purchased from BioLegend (San Diego, CA, USA). The mouse regulatory T cell staining kit (clone FJK-16s) and anti-mouse monoclonal antibody for IFN- $\gamma$  (clone XMG1.2) were obtained from eBioscience (San Diego, CA, USA). Mouse IFN- $\gamma$ , IL-4 and TNF- $\alpha$  ELISA kits were purchased from Beijing DAKWE Biotechnology Co., Ltd. The alanine aminotransferase kit (C009-2) and blood urea nitrogen test kit (C013-1) were purchased from the Nanjing Jiancheng Bioengineering Institute. Anti-PD-1 (clone RMP1-14) and anti-CTLA-4 (clone 9H10) monoclonal antibodies were obtained from Bioxcell (West Lebanon, NH, USA). GM-CSF (315-03) was acquired from PeproTech Inc. (Rocky Hill, NJ, USA). CCK-8 was bought from Dojindo (Shanghai, China). The lactate dehydrogenase (LDH) activity assay kit was received from Thermo Fisher Scientific (Waltham, MA, USA).  $\alpha$ -Amino- $\omega$ -methoxy poly (ethylene glycol) (mPEG-NH<sub>2</sub>,  $M_n$  = 2000 g/mol) was purchased from Sigma (St. Louis, MO, USA). L-alanine N-carboxyanhydride (Ala-NCA) was provided by Chengdu Enlai Biological Technology Co., Ltd. (Chengdu, Sichuan, China).

### **Synthesis and characterization of poly (ethylene glycol)-block-poly(L-alanine) copolymer**

mPEG-*block*-poly(L-alanine) (PEA) copolymer was prepared by the ring-opening polymerization (ROP) of L-Ala-NCAs using mPEG-NH<sub>2</sub> as the initiator according to the previously reported method [51, 52]. Briefly, mPEG-NH<sub>2</sub> and Ala-NCAs were dissolved in anhydrous dimethyl formamide. The solution was heated at 40°C for 24 h and the obtained crude products were added dropwise into cold anhydrous diethyl ether. The precipitate was filtrated and washed by diethyl ether for three times. Finally, the PEA copolymer was dried in vacuum. The chemical composition of PEA was determined by <sup>1</sup>H NMR (Varian Unity, 500 MHz, Varian Medical Systems, Inc., Palo Alto, CA, USA). The secondary structure was also examined by circular dichroism (CD, Jasco J-815) spectroscopy within the temperature range of 10–60°C.

### **Fabrication and characterization of vaccine- and inhibitor-encapsulated hydrogel**

First, the tumor antigen, TCLs was prepared. B16 cells were digested by trypsin, centrifuged, and resuspended in PBS at a density of 10<sup>7</sup> cells/mL. The

suspension was subjected to five cycles of rapid freezing in liquid nitrogen and thawing (37°C) and then centrifuged at 2000 rpm for 10 min. The supernatant containing TCLs was collected and lyophilized. Protein concentrations were measured by BCA assay to quantify the amount of TCLs. To prepare the hydrogel-based vaccine formulation, PEA copolymers were dissolved in PBS (100 mg/mL), which was followed by gentle sonication for 30 min. Afterwards, immunomodulation factors, including TCLs (500  $\mu$ g/mL), GM-CSF (3  $\mu$ g/mL), and individual anti-CTLA-4 (3 mg/mL), individual anti-PD-1 (3 mg/mL) antibody, or both antibodies were added to the polymer solution and the mixture was treated by mild sonication for 1 h to form a homogeneous hydrogel vaccine formulation. Rheological measurement by an AR 2000ex rheometer was implemented to study the mechanical properties of the hydrogels before and after cargo encapsulation. Three samples were prepared and each was tested for three or more times. Representative results were shown. The interior microstructure of the PEA hydrogel with or without these macromolecules was observed by a scanning electron microscope (SEM, S-4800, Hitachi, Japan) after rapid quenching in liquid nitrogen and lyophilization.

### **Cell viability assay**

To evaluate the potential cytotoxicity of PEA copolymer, CCK-8 assay of splenocytes, and bone marrow-derived dendritic cells (BMDCs) was performed within a polymer concentration range of 0 to 320  $\mu$ g/mL. Cells were seeded in a 96-well plate at a density of 1  $\times$  10<sup>5</sup> cells/cm<sup>2</sup>. Polymers were solubilized in culture media (RPMI 1640 Medium with 10% bovine calf serum) and after incubating for 24 h, the CCK-8 solution (10  $\mu$ L, 10% v/v in medium) was added to each well of the plate. 1 h later, the absorbance value at 450 nm was measured by a microplate reader (Bio-Rad Model 550, Bio-Rad Laboratories (Shanghai) Co., Ltd., Shanghai, China). Cell viability (%) was determined by calculating the absorbance ratio between the sample and the control group. All experiments were performed in triplicate. Moreover, the cytotoxicity towards BMDCs of hydrogels loaded with TCLs (500  $\mu$ g/mL), GM-CSF (3  $\mu$ g/mL), and anti-PD-1 antibody (3 mg/mL) alone or in combination with anti-CTLA-4 (3 mg/mL) antibody was also measured by LDH assay following the manufacturer's instructions.

### **Hydrogel swelling and controlled release of immunomodulation factors**

For the hydrogel swelling test, a given mass of hydrogel was placed in a centrifuge tube and the mass

was designated as M1. Ultrapure water (200  $\mu$ L) was added on the upper layer of the gel, and the centrifuge tube was gently shaken in a 37°C environment. At specific time points, the ultra-pure water was poured off and the mass of the centrifuge tube was designated as Mn. The swelling ratio was calculated by the formula:  $(Mn-M0)/(M1-M0)$ , where M0 was the mass of blank tube. Three parallel samples were used at each time point.

For the drug release study, copolymer aqueous solutions (100  $\mu$ L) loaded with TCLs (500  $\mu$ g/mL) and GM-CSF (3  $\mu$ g/mL) were placed in a 48-well plate in an incubator (37°C) for 30 min to form hydrogels. Then, 200  $\mu$ L PBS (pH 7.4, 0.01 M) was added to the top of each hydrogel. At scheduled time points, all of the release media were collected and replaced by fresh PBS. The concentration of TCLs and GM-CSF in the collected medium was determined by a MicroBCA™ protein assay kit and Mouse GM-CSF ELISA MAX™ Deluxe Set (B236567, BioLegend), respectively. The same procedure for the release of anti-PD-1 or anti-CTLA-4 antibody from the PEA hydrogel containing 3 mg/mL antibody was implemented and the concentration of antibodies was quantified by ELISA. The ELISA plates (Costar, Corning, New York, USA) were coated with mouse recombinant PD-1 protein (M5228, ACRO Biosystems, Beijing, China) or CTLA-4 protein (M52H5, ACRO Biosystems) following the manufacturer's instructions. Three parallel wells of each sample were determined. The accumulative release was calculated and the results were determined as the mean  $\pm$  standard deviation (SD).

### Generation of BMDCs and *in vitro* activation of DCs

BMDCs were generated from the hind limb bones of the mice according to previously described procedures [53, 54]. To determine DC activation by the hydrogel-based vaccine,  $2 \times 10^6$ /mL cells were cultured in RPMI 1640 supplemented with 10% FBS, 2 mmol/L L-glutamine, 1 mmol/L sodium pyruvate, 100 U/mL penicillin, 100  $\mu$ g/mL streptomycin, 20 ng/mL of GM-CSF (PeproTech) and 10 ng/mL of IL-4 (PeproTech) in 6-well plates. On day 5, obtained DCs were gently added to the upper layer of a transwell culture plate and 200  $\mu$ L of blank hydrogel or hydrogel-based vaccine (TCLs, 100  $\mu$ g; GM-CSF, 3  $\mu$ g) was added at the bottom. DCs without any treatment were used as controls. Two days later, cells in the insert upper layer and those having entered the hydrogel were harvested and labeled by CD11c and MHCII antibodies (eBioscience), which were then analyzed by flow cytometry (BD Accuri™ C6, BD Biosciences, San Jose, CA).

### *In vivo* cell recruitment and secretion of antibody and cytokines

Female C57BL/6J mice (6–8 weeks old) were received subcutaneous injections of 100  $\mu$ L blank hydrogel or hydrogel encapsulated with TCLs (500  $\mu$ g/mL) and GM-CSF (3  $\mu$ g/mL). To visualize the overall cell recruitment within the hydrogels, mice were killed 4 days post-injection, and hydrogels were explanted and embedded in optimal cutting temperature (OCT) compound, followed by sectioning and staining with hematoxylin and eosin (H&E) for histological analysis. Furthermore, the total number of cells within the hydrogel was also counted by an automated cell counter (Countstar® IC1000, Shanghai Ruiyu Biotech Co. Ltd., Shanghai, China).

To detect the antibody levels, C57BL/6 mice were immunized with vaccine formulations. On day 14, 50  $\mu$ L of blood was obtained from the eye canthus, and the level of IgG was measured by ELISA (Mouse IgG ELISA Kit, Bethyl Laboratories, Inc., Montgomery, TX, USA). For cytokine detection, peripheral blood was taken from the treated mice and serum was collected for IFN- $\gamma$ , IL-4, and TNF- $\alpha$  analysis by ELISA (eBioscience).

### *In vivo* identification of DCs and T cells

The blank hydrogel or the hydrogel vaccines containing 100  $\mu$ g of TCLs in combination with 3  $\mu$ g of GM-CSF were injected subcutaneously into the left flanks of 6-week-old female C57BL/6J mice. At various time points post-injection, the hydrogels and spleens were extracted and digested and the cells were isolated. To assess DC infiltration and activation in the hydrogel, the isolated hydrogels were diluted by 4 mL PBS into solutions, which were poured through a 40- $\mu$ m cell strainer to isolate the polymer aggregates and cells. The recovered cells were pelleted, washed with cold PBS and then stained with primary antibodies conjugated with fluorescent markers (2.5  $\mu$ g/mL) to allow for flow cytometry analysis. Percp-Cy5.5-conjugated CD11c was used to stain DCs, and APC-conjugated CD86 staining was conducted to evaluate the maturation of DCs.

To assess T-cell infiltration and activation, spleens were excised and single cell suspensions were prepared. Briefly, spleens were homogenized and filtered through a 70- $\mu$ m cell strainer. The suspended cells were transferred to a 15-mL centrifuge tube with 4 mL Ficoll, and then covered with 1 mL RPMI 1640 medium and centrifuged with a discontinuous Ficoll gradient at 800 g for 30 min. T cells were collected from the interphase and washed. FITC-conjugated CD3 and PE-conjugated CD8a antibodies were used to label T cells, which were then analyzed by flow cytometry.

### **In vitro cytotoxic T lymphocyte (CTL) assay**

CTL-mediated cytotoxicity to melanoma cells *in vitro* was tested by a CTL assay kit (Promega, Madison, Wisconsin, USA). C57BL/6J mice were vaccinated with blank hydrogels, hydrogels loaded with TCLs (500 µg/mL) and GM-CSF (3 µg/mL) (denoted as Vaccine), hydrogels loaded with Vaccine and individual anti-PD-1 antibody (3 mg/mL) (denoted as Vaccine + αAnti-PD-1) or anti-CTLA-4 antibody (3 mg/mL) (denoted as Vaccine + αAnti-CTLA-4), or both antibodies (Vaccine + αAnti-PD-1 + αAnti-CTLA-4). The spleens were collected on day 7 after the administration of various formulations. Single cell suspensions of T lymphocytes were prepared and denoted as CTL effector (E) cells. B16 melanoma cells were indicated as target (T) cells. Effector and target cells were co-incubated in 96-well flat bottom plates with E/T cell ratios ranging from 10:1 to 50:1 for 4 h at 37°C in a 5% CO<sub>2</sub> environment. Then, the level of lactate dehydrogenase was tested by CTL assay kit following the manufacturer's instructions.

### **Therapeutic efficacy and analysis of T cell subpopulations in tumors and spleens**

Female C57BL/6J mice (6–8 weeks old, n=8 for each group) were given subcutaneous injections of 10<sup>5</sup> B16 melanoma or 4T-1 tumor cells into the left flanks. At day 7, 100 µL blank PEA hydrogel or PEA hydrogel-based vaccines containing melanoma TCLs (500 µg/mL) and GM-CSF (3 µg/mL) plus either anti-PD-1 (3 mg/mL), and anti-CTLA-4 (3 mg/mL) antibody, or both inhibitors were subcutaneously injected at the site of upstream relative to the lymphatic draining. Mice without any treatment were set as the control group. Mice were closely monitored every other day for tumor growth and body weight. Tumor growth was measured using a digital caliper by blinded investigators and calculated according to the following equation: tumor volume (mm<sup>3</sup>) = 0.5 × length (mm) × width<sup>2</sup> (mm<sup>2</sup>). Mice were killed when the tumor volume exceeded 2000 mm<sup>3</sup> and tumors were removed and weighed. B16 cell apoptosis within the tumor tissues was indicated by TUNEL staining (Beyotime Biotechnology, Shanghai, China) according to the manufacturer's instructions.

The spleens were excised to analyze T cell subpopulations. After tissue treatment and cell separation, isolated T lymphocytes were stained with fluorescence-conjugated antibodies against mouse CD3, CD4, or CD8. After surface staining, the cells were permeabilized, fixed, and stained with IFN-γ before analysis of CD8<sup>+</sup>/CD4<sup>+</sup>IFN-γ<sup>+</sup> T cells by flow cytometry.

Tumor infiltrating lymphocytes (TILs) were also harvested. Briefly, tumor tissues were separated, cut into small pieces, put into a dish containing Ficoll, and then centrifuged with a discontinuous Ficoll gradient. TILs were collected from the interphase, washed, and then stained with IFN-γ-FITC and FoxP3-APC antibodies to analyze IFN-γ<sup>+</sup>CD8<sup>+</sup> T cells by flow cytometry.

The inguinal draining lymph nodes (dLNs) were also excised and processed into single cell suspensions. The isolated cells were stained with PerCP-Cy5.5-conjugated CD11c, APC-conjugated CD86 and FITC-conjugated CD40 antibodies for identifying the phenotype of DCs by fluorescence-activated cell sorting (FACS) analysis. T lymphocytes were also stained with FITC-conjugated CD4 and APC-conjugated FoxP3 antibodies to analyze Tregs.

### **Statistical analysis**

All animal studies were performed with randomization and data were analyzed by unpaired two-tailed Student's *t*-test to indicate statistically significant differences between two groups by Prism 6 (GraphPad Software, Inc., La Jolla, CA, USA). Multiple comparisons were performed where there was more than two groups being compared, or where data was collected over time, by one-way ANOVA. *P*<0.05 was considered to be statistically significant. All values are presented as means ± SDs unless indicated otherwise.

## **Results**

### **Preparation and characterization of PEGylated polypeptide hydrogels and formulations**

mPEG-*b*-poly(L-alanine) (PEA) copolymer was first prepared by ROP of L-Ala NCAs using mPEG-NH<sub>2</sub> as the initiator. The <sup>1</sup>H NMR spectrum (Figure S1A) was recorded to investigate the composition and the number-average molecular weight (*M<sub>n</sub>*) of PEA. The integration ratio of the characteristic peak at 3.65 ppm attributed to the hydrogen protons of methylene on the PEG segment and that at 4.4 ppm assigned to the hydrogen proton of methane on the poly(L-alanine) block were used to calculate the degree of polymerization of L-alanine, which was approximately 10. Thus, the molecular weight of PEA copolymer used in this study was 2710 g/mol. The physicochemical characteristics of PEA were summarized in Table S1 and its chemical formula was shown in Figure 1A. PEA was dissolved in water at a concentration of 100 mg/mL and self-assembled into a hydrogel. The secondary



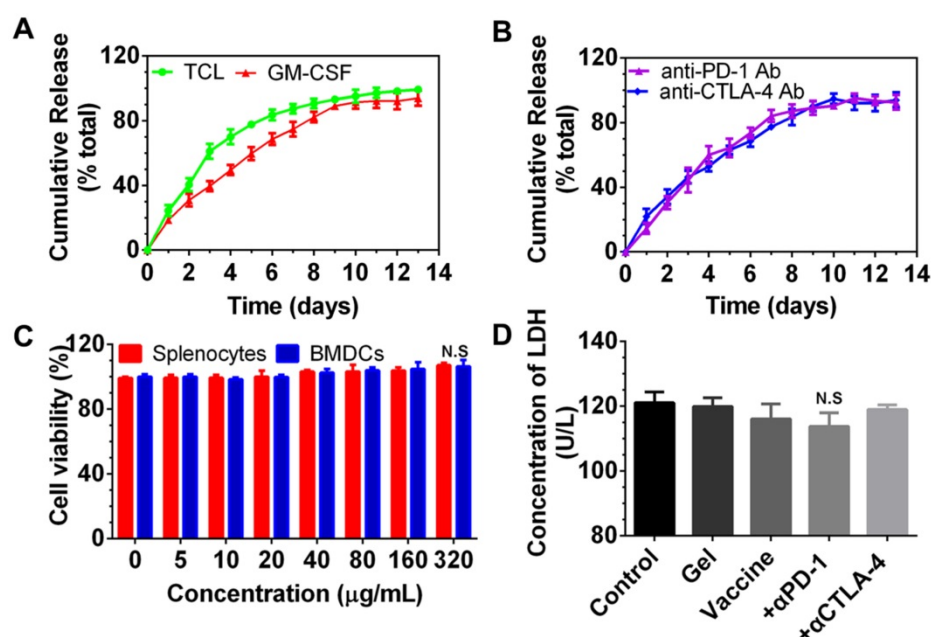


**Figure 2. Cumulative release of immunomodulators from the PEA hydrogel and *in vitro* cytotoxicity of PEA copolymer and hydrogel-based formulations on splenocytes and BMDCs.** (A, B) Release profiles of TCLs, GM-CSF, and anti-PD-1/CTLA-4 antibodies (Ab). Content of each factor released in the medium was determined by the corresponding ELISA kits. Data are shown as mean  $\pm$  SDs (n=3). (C, D) The cytotoxicity effect of the PEA copolymer on splenocytes (C) and BMDCs (D). N.S. = not significant ( $p > 0.05$ ), versus the control and other groups. Cells were treated with the copolymer for 24 h, and the cytotoxicity was measured using a CCK-8 kit. (E) Results of LDH assay. BMDCs were treated with PBS (control), blank hydrogels (gel), hydrogels delivering TCL with GM-CSF (referred to as the vaccine), or vaccines with anti-PD-1 ( $+\alpha$ -PD-1) alone or in combination with anti-CTLA-4 antibodies ( $+\alpha$ -CTLA-4). Bars shown are mean  $\pm$  SDs (n= 3).

### Controlled release of immunomodulators, cytotoxicity analysis, and DC recruitment and activation *in vitro*

After encapsulation, we examined whether these immunomodulators can be released from the PEA hydrogel. As shown in Figure 2A and 2B, PEA hydrogel provided sustained release of TCLs, GM-CSF, and immunological checkpoint inhibitors. Approximately 83.70% and 89.16% of the total TCLs and GM-CSF were released within the first 6 and 9 days, respectively, and slow release was followed over the next 7 and 4 days. In addition, Figure 2B shows that both anti-PD-1 and anti-CTLA-4 antibodies were also released in a sustained manner. Complete release occurred after approximately 10 days.

Next, the cytocompatibility of PEA copolymer was assessed by determining the viability of splenocytes and BMDCs treated with PEA. As presented in Figure 2C, cell viability upon exposure to the PEA copolymer was around 100% within the concentration range of 1 to 320  $\mu$ g/mL in the medium, demonstrating that the PEA was nontoxic and compatible with these cells. BMDCs were then cultured with hydrogel-based vaccine formulations alone or supplemented with antibodies for 24 h, and the content of LDH in the culture medium was determined. Figure 2D indicates that there was no significant difference between treatment with the hydrogel vaccines, the vaccines in combination with

antibodies, and the control group, suggesting that vaccines are compatible with DCs. These results prove that PEA copolymer, blank PEA hydrogel, and the hydrogel encapsulated with immunomodulators have good cytocompatibility with DCs.

Then, whether the sustained release of TCLs and GM-CSF can activate DCs was studied *in vitro*. BMDCs were cultured with blank hydrogels or hydrogel vaccine. Two days later, BMDCs were stained by CD11c and MHCII antibodies. Figure S2 indicates that in comparison with the control or the blank hydrogel group, co-delivery of tumor antigens and GM-CSF by the PEA hydrogel significantly induced the maturation of BMDCs, as demonstrated by the much higher percentage (>40%) of CD11c<sup>+</sup>MHCII<sup>+</sup> DCs.

### Recruitment and activation of DCs by the hydrogel-based vaccine *in vivo*

As described above, the PEA hydrogel-based vaccine could efficiently activate DCs *in vitro*, and the porous structure of hydrogel may allow for the infiltration of inflammatory cells *in vivo*. Vaccine was injected into the subcutaneous site of C57BL/6J mice. Histological analysis (Figure 3A) at day 4 after injection revealed extensive cell infiltration compared to the blank hydrogel controls and over  $6 \times 10^6$  cells were collected into the hydrogel. H&E staining can distinguish various inflammatory cells by cell morphology and size. Lymphocytes are commonly

small and round, and their nucleoplasmic ratio is large. Moreover, their nucleus is densely stained in dark blue violet. Monocytes are the largest leukocytes and their nucleus often appear in pleomorphic shapes including oval, kidney-shaped, horseshoe, and irregular shapes. The chromatin is loosely reticulated with light coloration, while the cytoplasm is dyed in grayish-blue due to the large number of small azurophilic granules. According to these criteria, the cells present in the hydrogel vaccine were mainly lymphocytes and monocytes. Furthermore, the activation of DCs which were the highest proportion of professional APCs within the hydrogel as a function of time was analyzed by identifying their phenotype. The co-stimulatory molecule CD86 was used as a marker of DC maturation. Flow cytometry analysis (Figure 3B) demonstrated that 4 days after vaccine injection, approximately 14.4% of the DCs recruited were CD11c<sup>+</sup>CD86<sup>+</sup>, which was equal to

about  $9 \times 10^5$  cells. At day 9, the percentage of activated DCs significantly increased to 27.4% before falling to 17.4% on day 13. This result indicates that the hydrogel vaccine was able to sustainably recruit and activate DCs.

Next, the antigen-specific humoral and cellular responses were examined by detecting the antibody titer, and cytokine and splenic CD8<sup>+</sup> T cells. ELISA results (Figure 4A-D) indicated that vaccination with the hydrogel vaccine produced a significantly higher level of IgG expression compared with the control or with the blank hydrogel, indicating a stronger humoral response. Moreover, the secretion of T-cell-derived cytokines including IFN- $\gamma$  and IL-4, and pro-inflammatory cytokines such as TNF- $\alpha$  in plasma were also upregulated with the treatment of hydrogel vaccines, which demonstrated the occurrence of Th-based cellular responses. Furthermore, to elucidate the adaptive immunity

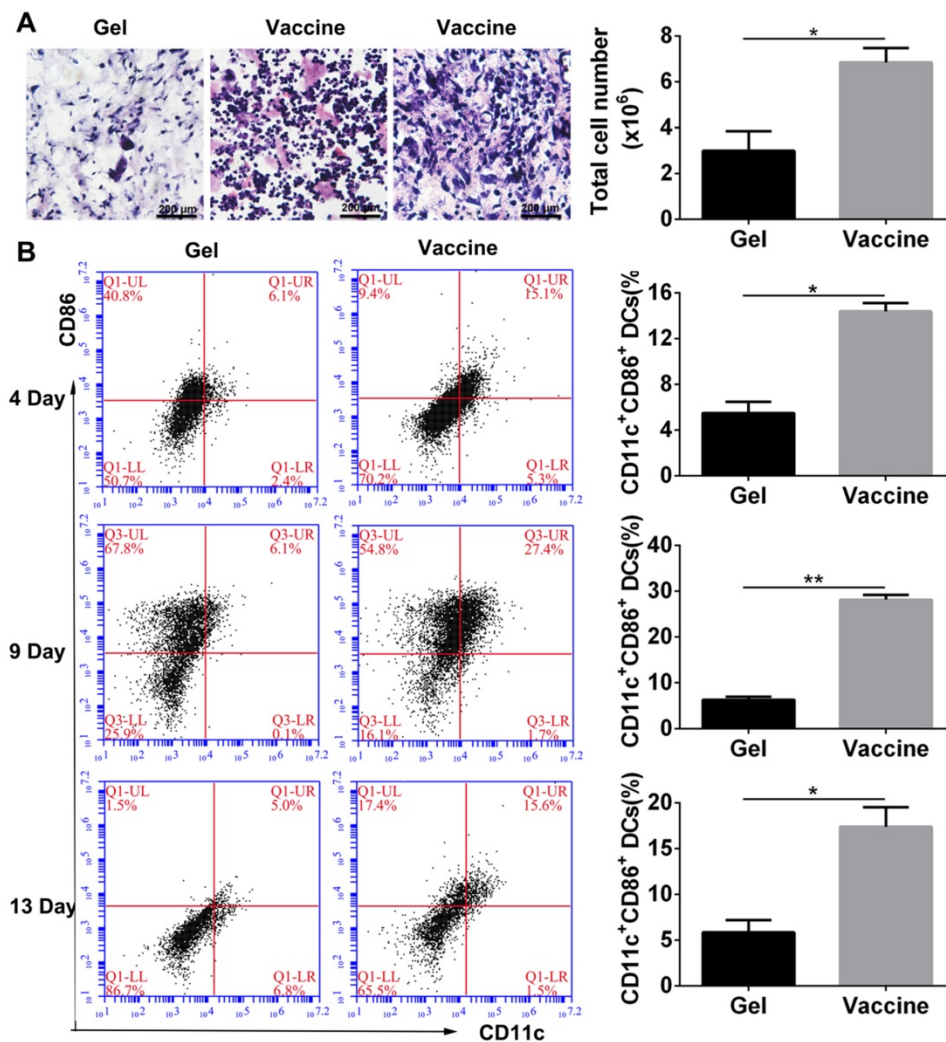


**Figure 3.** *In vivo* cell infiltration and recruitment and activation of DCs by the administration of polypeptide hydrogel vaccine. (A) Representative H&E staining images of the sectioned PEA hydrogel explanted from back subcutaneous pockets of C57BL/6J mice at 4 days post-hydrogel injection. Lymphocytes and monocytes were indicated by red and black arrow, respectively. Cells within hydrogels were also counted by an automated cell counter and the results are shown as mean  $\pm$  SDs (n=3). (B) Percentage of CD11c<sup>+</sup>CD86<sup>+</sup> DCs inside the hydrogel containing both TCLs and GM-CSF over time. At predetermined times, the hydrogels were excised and the cells were separated and stained by CD11c and CD86, which then subjected to flow cytometry analysis. Data are shown as mean  $\pm$  SDs (n=5). \*P<0.05 and \*\*P<0.01 versus blank hydrogels.

induced by the PEA hydrogel vaccine, the activity of systemic CTLs was examined. The stimulation and persistence of the systemic CTL response was monitored by staining splenocytes with CD3 and CD8 antibodies to identify the CD3<sup>+</sup>CD8<sup>+</sup> T cells. As shown in Figure 4E, at day 4, a significant expansion of CD3<sup>+</sup>CD8<sup>+</sup> T cells was observed in the spleens of mice vaccinated by the hydrogel co-delivering T cells and GM-CSF. The proportion of CD3<sup>+</sup>CD8<sup>+</sup> T cells in spleens continued to increase, and thereafter

decreased at day 13. These results suggest that the priming of systemic anti-melanoma antibodies and cellular responses can be efficiently accomplished and sustained for extended time periods by the administration of the PEA hydrogel-based vaccine.

**In vivo combinatorial immunotherapy and in vitro CTL assay**

Since the hydrogel vaccine was able to induce the CTL response *in vivo*, melanoma tumor-bearing

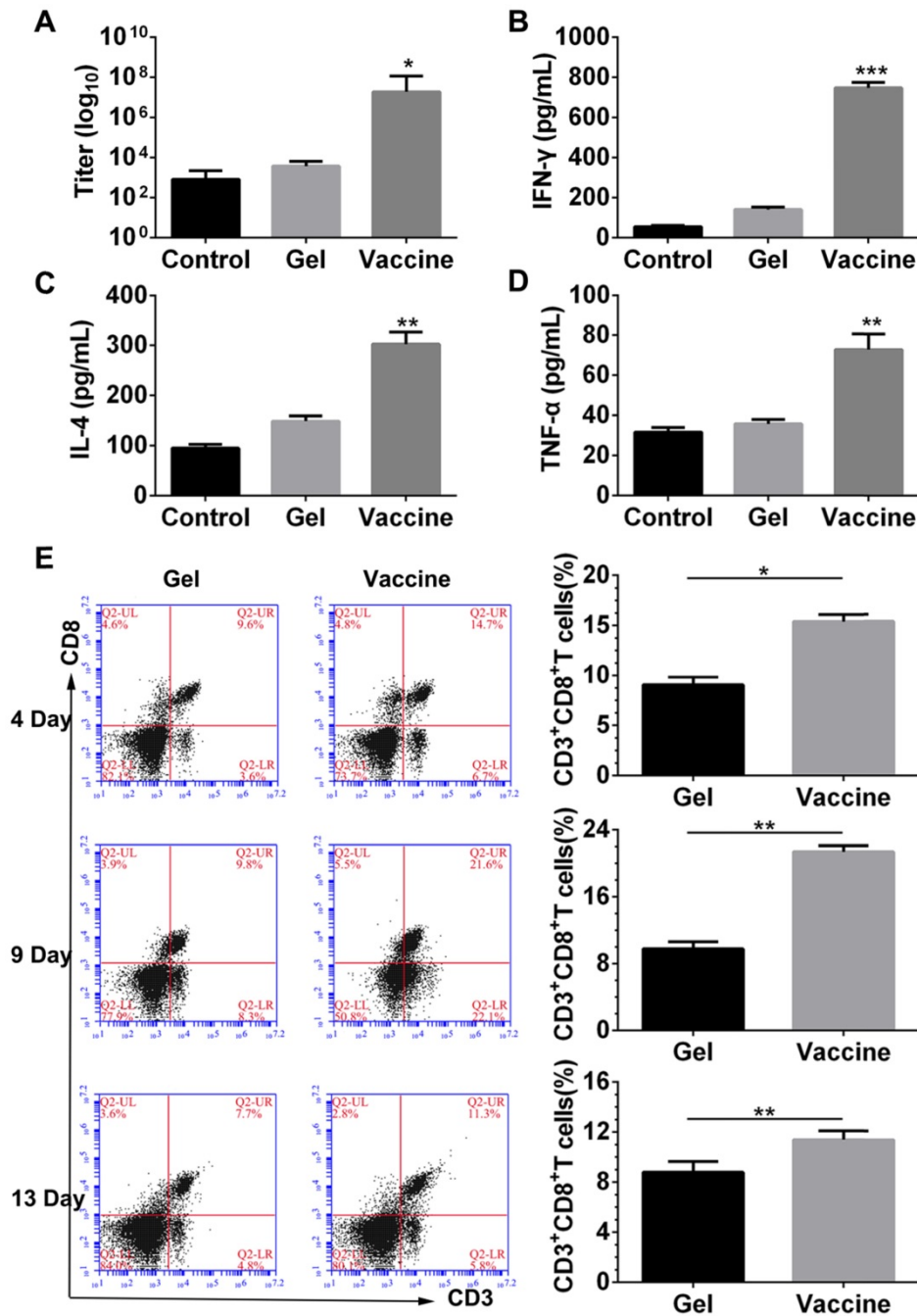


**Figure 4. Antibody titer, cytokine secretion and priming of systemic CD8<sup>+</sup> T-cell response induced by the hydrogel vaccine.** (A-D) The level of IgG (A) and cytokines, including IFN-γ (B), IL-4 (C), and TNF-α (D), in the serum from mice immunized with blank hydrogel or vaccine. \*P<0.05, \*\*P<0.01 and \*\*\*P<0.001 versus blank hydrogels. (E) Time-dependent change of the percentage of CD3<sup>+</sup>CD8<sup>+</sup> T cells in the spleens of immunized mice. Splenocytes were isolated, stained by CD3 and CD8 antibodies, and analyzed by flow cytometry. Data are shown as mean ± SDs (n=5). \*P<0.05, and \*\*P<0.01, versus blank hydrogels.

mice were given injections of hydrogel vaccine with or without checkpoint inhibitors to study *in vivo* antitumor efficiency. Prior to this, the immunotherapeutic efficacy of the tumor vaccine and inhibitors combined in solution or in the hydrogel was compared, and the results (Figure S3) indicated that hydrogel-based co-delivery of the vaccine and inhibitors resulted in significantly better tumor growth inhibition and lower tumor mass, which highlights the usefulness of the hydrogel-based drug delivery. At 7 days post-subcutaneous inoculation with B16 melanoma cells, mice were randomly divided into six groups and immunized once with the hydrogel vaccine containing TCLs and GM-CSF (Vaccine) or its combination with anti-PD-1 antibody alone (Vaccine +  $\alpha$ PD-1), anti-CTLA-4 antibody alone (Vaccine +  $\alpha$ CTLA-4), or with both antibodies (Vaccine +  $\alpha$ PD-1 +  $\alpha$ CTLA-4). As indicated by the tumor volume curves depicted in Figure 5B, Vaccine +  $\alpha$ PD-1 +  $\alpha$ CTLA-4 significantly delayed the growth of melanoma tumors compared to the other groups, while mice immunized by either Vaccine +  $\alpha$ PD-1 or Vaccine +  $\alpha$ CTLA-4 also exhibited slower tumor development compared to that of the Vaccine group. This result indicates that the combination immunotherapy was superior in suppressing melanoma tumors. The Vaccine +  $\alpha$ CTLA-4 group showed slightly better tumor inhibition compared to Vaccine +  $\alpha$ PD-1. All treatments were safe and without toxicity as suggested by the increase in mouse

body weight (Figure 5C). The weights of tumors (Figure 5D) excised at day 25 also showed that the Vaccine +  $\alpha$ PD-1 +  $\alpha$ CTLA-4 significantly decreased the tumor weight.

The specific lysis of melanoma cells was examined by a CTL assay. Effector cells (Effector), splenocytes isolated from the vaccinated mice were co-incubated with the target cells (Target), which were B16 melanoma cells. The cell ratio of Effector/Target was in the range of 10:1 to 50:1. LDH released from the cells was determined and Figure 5D clearly shows that the lysis of B16 melanoma cells was dependent on the Effector/Target cell ratio. Significantly, effector T cells from mice vaccinated with the hydrogel encapsulated with vaccine and dual inhibitors lysed ~55% of melanoma cells at an Effector/Target cell ratio of 50:1, which is significantly higher than for the other groups. These data illustrate that the hydrogel-based co-delivery of the tumor vaccine and double checkpoint inhibitors was much more efficient in evoking a potent melanoma-specific CTL response.

Cell apoptosis examined by TUNEL assays (Figure 6) further revealed that the combinatorial immunotherapy resulted in a significantly higher level of tumor cell apoptosis. Effective inhibition of 4T-1 tumors (Figure S4) was also obtained by the hydrogel-based vaccination and checkpoint blockade, which showed increased percentage of CD4<sup>+</sup>, CD8<sup>+</sup>, and IFN- $\gamma$ <sup>+</sup>CD8<sup>+</sup> T cells in the spleen (Figure S5, Figure S6A) and an increased ratio of IFN- $\gamma$ <sup>+</sup>CD8<sup>+</sup> T cells to Tregs (Figure S6B and 6C). In addition, CD8<sup>+</sup> T cells (Figure S7) within lymph nodes were also apparently primed. These data indicate that hydrogel-based co-delivery of the vaccine and immune checkpoint inhibitors is a better immunotherapy approach against melanoma and 4T-1 tumors.

### **In vivo analysis of effector T cell phenotypes in spleens and tumors**

We next examined effector T cells within spleens and tumors to explore how the combination immunotherapy works. After tissue treatment and antibody staining, cells were analyzed by flow cytometry. Figure 7A indicated that the hydrogel vaccine induced a significant

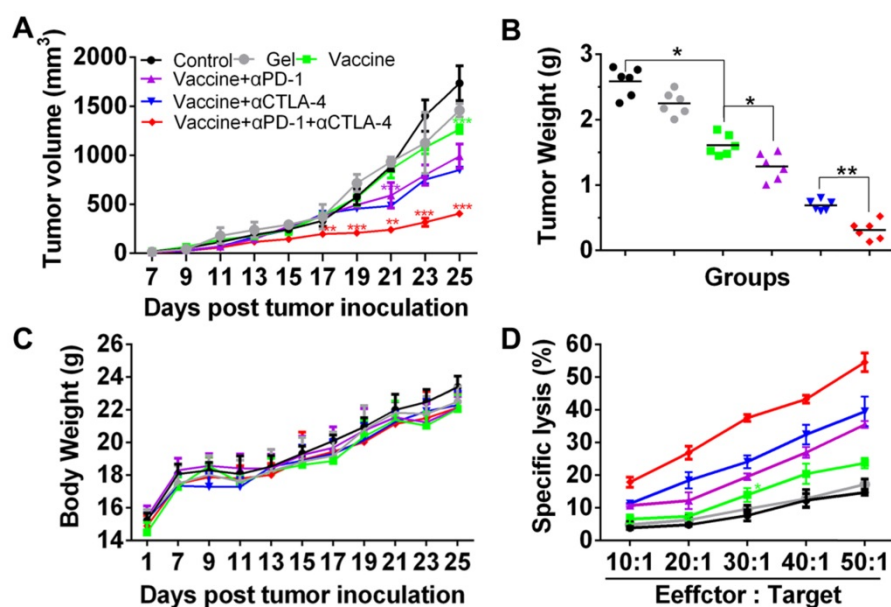


**Figure 5. Hydrogel-based co-delivery of vaccine and dual checkpoint inhibitors induced potent therapeutic efficiency against B16 melanoma.** (A) The curve of tumor volumes. Data are shown as mean  $\pm$  SDs (n=6). The statistical difference between Vaccine and Control, Vaccine+ $\alpha$ PD-1 and Vaccine, or Vaccine+ $\alpha$ PD-1+ $\alpha$ CTLA-4 and Vaccine+ $\alpha$ CTLA-4 group was calculated by using two-way ANOVA in GraphPad Prism software, which was labeled in green, purple and red asterisk, respectively; \* $P$ <0.05, \*\* $P$ <0.01, and \*\*\* $P$ <0.001. (B) Mass weight of tumors excised at day 25. \* $P$ <0.05, and \*\* $P$ <0.01, between indicated groups. (C) The profile of animal body weight post-tumor inoculation. (D) *In vitro* CTL assay at various Effector/Target cell ratios.

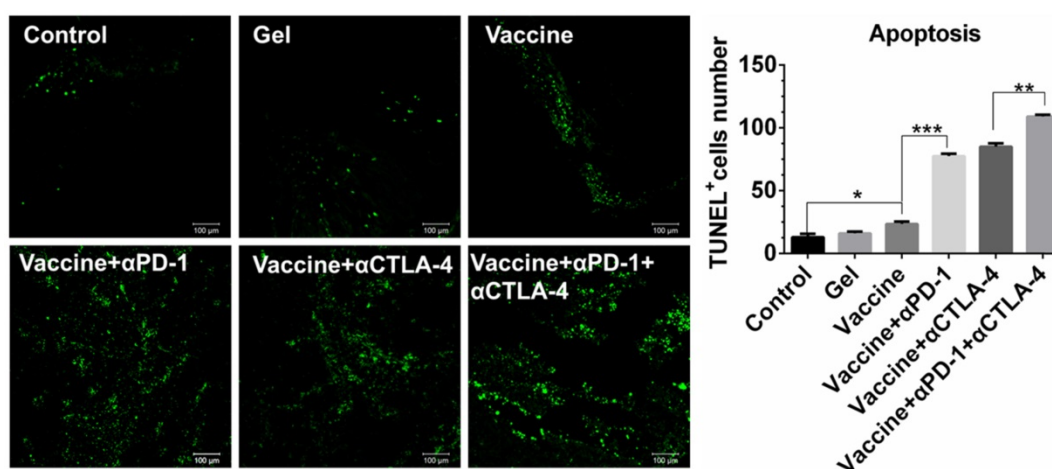


**Figure 6. Apoptosis of B16 melanoma cells within tumors.** Tumors were sectioned, stained by TUNEL agents, and observed by fluorescence microscope. The green color indicates the apoptotic cells, which were counted by Image J software. Data are shown as mean  $\pm$  SDs (n=4). \* $P$ <0.05, \*\* $P$ <0.01, and \*\*\* $P$ <0.001, between indicated groups.

expansion of CD3<sup>+</sup>CD8<sup>+</sup> cytotoxic T cells in spleens. The addition of either anti-PD-1 or anti-CTLA-4 treatment to the vaccination provided a 2.2-2.8-fold increase in the proportion of CD3<sup>+</sup>CD8<sup>+</sup> T cells, whereas the combinatorial addition of both inhibitors generated over a 4.4-fold increase. Significantly, the double inhibitor treatment along with the vaccine produced a 2-fold enhancement in the frequency of CD8<sup>+</sup> T cells in contrast to the individual blockade. Moreover, supplementing the vaccination with dual checkpoint inhibitors also resulted in an increase in the percentage of systemic cytotoxic and activated CD8<sup>+</sup> T cells (Figure 7B), as determined by the co-expression of IFN- $\gamma$ , which is a typical marker of CD8<sup>+</sup> T cell activation. A similar effect was found for the production of CD3<sup>+</sup>CD4<sup>+</sup> T cells (Figure 7C) as well as IFN- $\gamma$ -positive CD4<sup>+</sup> T cells (Figure 7D). CD4<sup>+</sup> T cells are important for assisting and maintaining the cytotoxicity T lymphocyte cell response. These findings suggest that combining PEA hydrogel vaccines with both PD-1 and CTLA-4 antibodies can dramatically enhance the percentage of activated effector T cells within the spleen, indicating that it can augment the antitumor T-cell immunity systemically.

Because the checkpoint blockade is supposed to improve the activity of effector T cells as well as reduce Tregs, we looked at the effects of combination therapy on the reduction of systemic Treg infiltration. FoxP3 antibody was used to stain Tregs followed by flow cytometry analysis (Figure 8A). All treatment groups showed a decrease in the fraction of Tregs in spleens when compared to the control group (Figure 8B), and the hydrogel vaccine in combination with both checkpoint inhibitors significantly reduced the proportion of Tregs in comparison with the vaccine alone or the vaccine with PD-1 blockade. In the case of activated CD8<sup>+</sup> T-cell-to-Treg ratios (Figure 8C), hydrogel vaccine therapy in combination with both

PD-1 and CTLA-4 blockades significantly increased the IFN- $\gamma$ <sup>+</sup>CD8<sup>+</sup> T/Treg ratios, in comparison with vaccine therapy or vaccine in addition with any individual antibody. These data suggest that the combinatorial immunotherapy preferentially enhanced effector T-cell generation and expansion over Tregs in spleens. Previous studies in mice have shown that anti-CTLA-4 monoclonal antibodies including ipilimumab, pembrolizumab, and tremelimumab, block the function of CTLA-4 and deplete intratumoral FOXP3<sup>+</sup> regulatory T cells via an Fc-dependent mechanism [58-60]. Studies in human tumors also suggest that anti-CTLA-4 efficacy can be enhanced by modifying the Fc portions of the monoclonal antibodies [61]. Another mechanism by which cancer limits the host immune response is via upregulation of PD-L1 and PD-L2 that is associated with PD-L1 expression [62-64]. The objective response to anti-PD-1 therapy is most closely correlated with tumor cell PD-L1 expression [63]. As a result, combining anti-PD-1 and anti-CTLA-4 therapy in the hydrogel should improve antitumor efficacy by augmenting effector T cell-mediated immune responses and inhibiting tumor immune resistance.

TILs are known to lyse tumor cells directly within tumor tissue. In the present study, tumor tissues were digested, then single-cell suspensions were prepared, which were then stained by antibodies and examined by flow cytometry. Results shown in Figure 9 indicate that the addition of dual checkpoint blockades significantly enhanced the percentage of total CD8<sup>+</sup> effector T cells that were activated (IFN- $\gamma$ -positive), indicating the hydrogel delivery system promoted local T-cell cytotoxicity within tumors. The proportion of IFN- $\gamma$ <sup>+</sup>CD8<sup>+</sup> T cells within the tumors was nearly as high as 20% with the combination treatment. We also attempted to analyze the Tregs within tumors, but unfortunately an

insufficient number of cells was obtained. As an alternative, we assessed DC activation and Tregs in the dLNs (Figure S9). The addition of checkpoint blockade to the hydrogel vaccine treatment significantly activated DCs in the dLNs as

demonstrated by the greater proportions of CD86<sup>+</sup> or CD40<sup>+</sup> CD11c<sup>+</sup> DCs, and the addition of double antibodies resulted in a superior effect on DC activation over all other treatments.

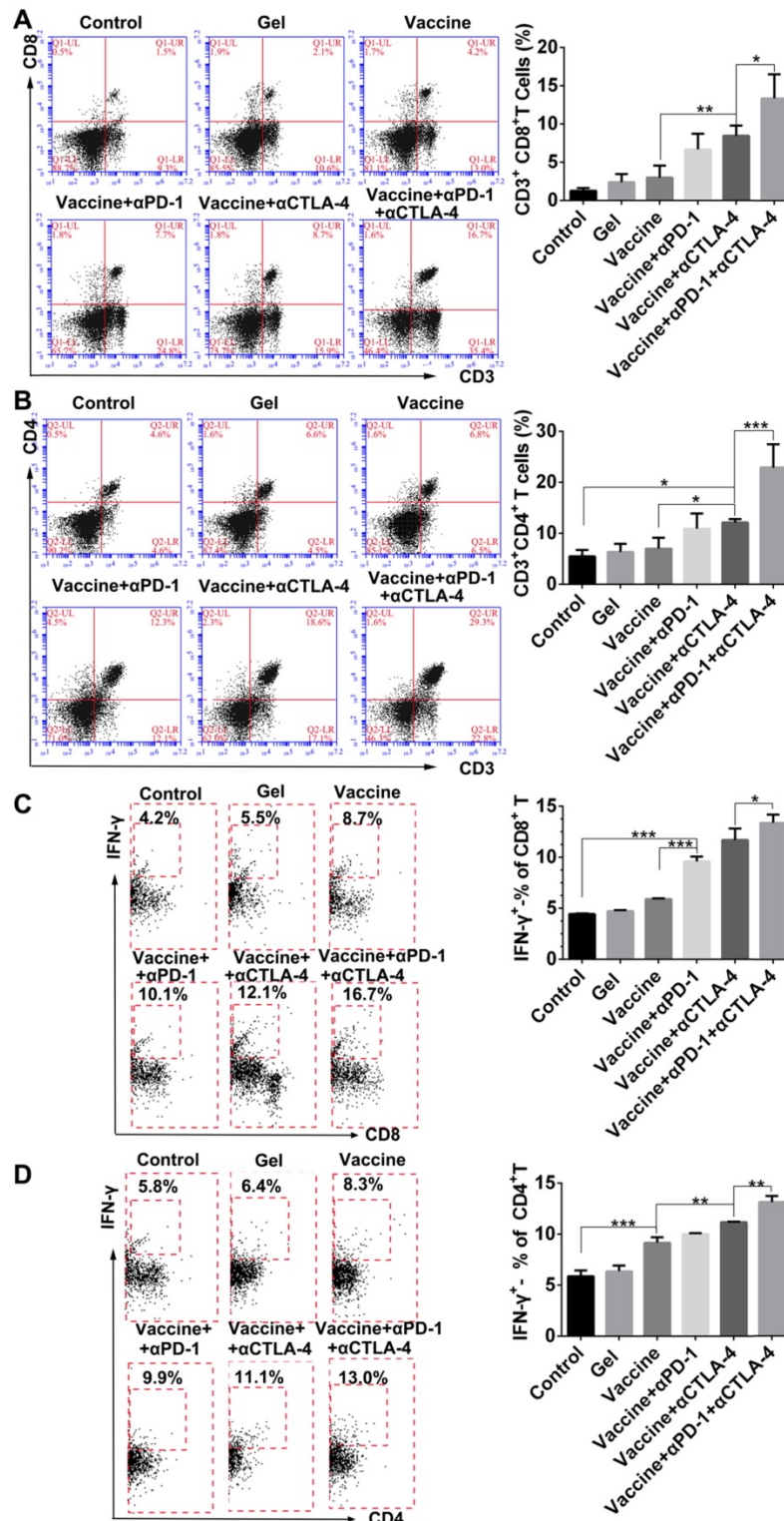


**Figure 7. Hydrogel-based co-delivery of vaccine and checkpoint inhibitors enhanced the systemic T-cell response.** (A, C) Ratio of CD8<sup>+</sup> T (A) or CD4<sup>+</sup> T (C) cells isolated from the spleens of untreated tumor-bearing mice (control) and mice treated with blank hydrogels (gel) or hydrogel vaccines (vaccine) alone, or in combination with either anti-PD-1 (+αPD-1) or anti-CTLA-4 (+αCTLA-4) antibodies or with dual antibodies (+αPD-1+αCTLA-4). (B, D) The ratio of IFN-γ<sup>+</sup>CD8<sup>+</sup> T (B) or IFN-γ<sup>+</sup>CD4<sup>+</sup> T (D) cells to the total number of CD8<sup>+</sup> T or CD4<sup>+</sup> T cells in the spleens as determined by flow cytometry. Data are shown as mean ± SDs (n=4). \*P<0.05, \*\*P<0.01 and \*\*\*P<0.001, between indicated groups.

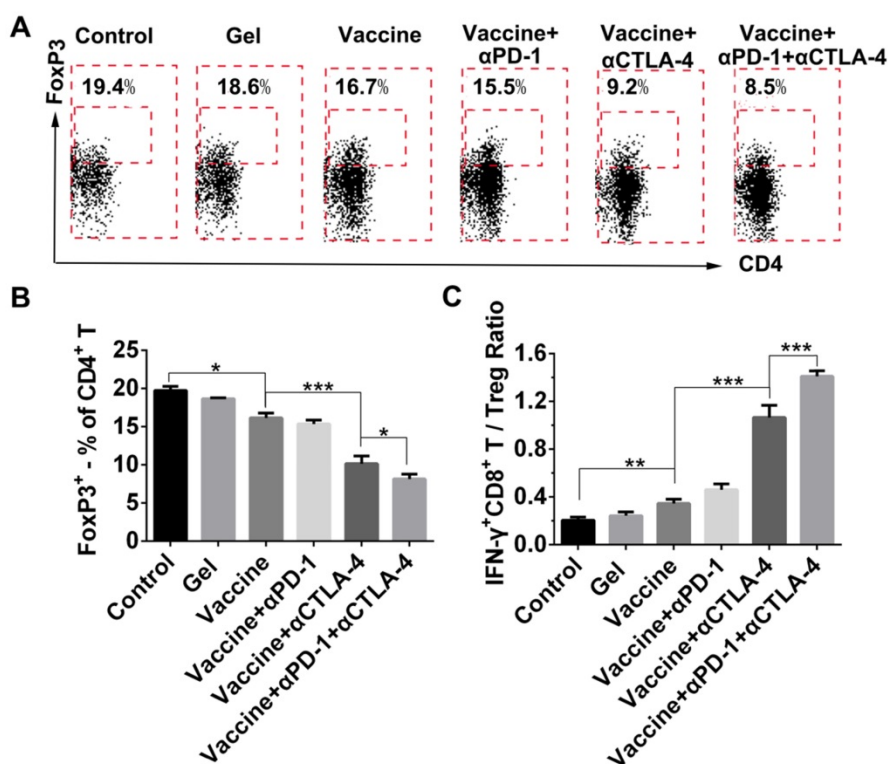


**Figure 8. Effect of combination therapy on reducing the presence of systemic Tregs.** (A) Representative flow cytometry profiles of FoxP3 and CD4 staining and (B) quantification analysis of FoxP3<sup>+</sup>CD4<sup>+</sup> T cells in the spleens. Original profiles of full dot plots are shown in Figure S8. (C) Ratios of IFN-γ<sup>+</sup>CD8<sup>+</sup> T cells to Tregs. Data are shown as mean ± SDs (n=4). \*P<0.05, \*\*P<0.01, and \*\*\*P<0.001, between indicated groups.

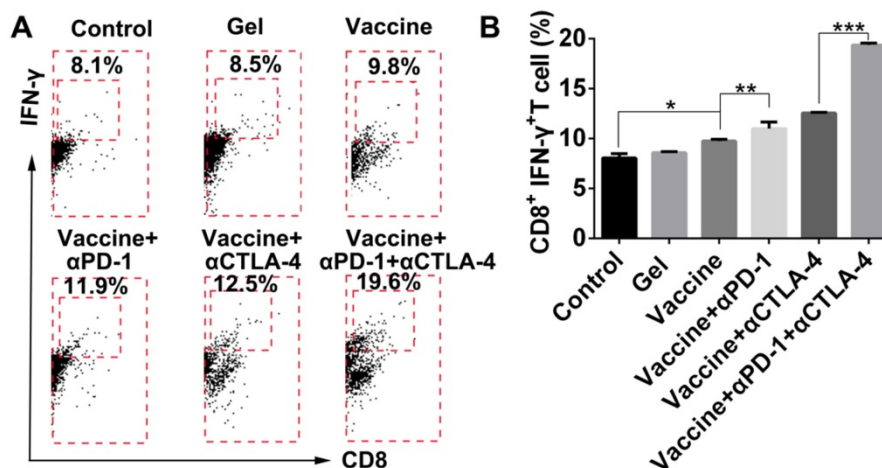


**Figure 9. Hydrogel-based co-delivery system promoted the expansion of tumor-infiltrating T lymphocytes (TILs).** (A) Representative flow cytometry profiles of IFN-γ and CD8 staining and (B) the quantification analysis of IFN-γ<sup>+</sup>CD8<sup>+</sup> T cells within tumors. Data are shown as mean ± SDs (n=4). \*P<0.05, \*\*P<0.01, and \*\*\*P<0.001, between indicated groups.

This phenomenon could be attributed to antibody blockade of PD-1 or CTLA-4 leading to higher T cell motility and activity, thereby, enhancing T cell-DC contacts and interactions [65]. Noticeably, supplementing vaccine with immune checkpoint blockade also significantly reduced the ratio of Tregs in dLNs. Additionally, it seemed that the vaccination supplemented with anti-CTLA-4 antibody conferred better systemic and tumoral effector CD8<sup>+</sup> T cell activation and infiltration in contrast to that with anti-PD-1 antibody; this was more obvious in spleens,

suggesting that PD-1 activity may dominate tumoral microenvironments, while CTLA-4 probably affected a larger range of systemic T lymphocytes.

### Discussion

Over the past decade, vaccines and immune checkpoint blockades have emerged to harness the immune system to treat cancers. Because each approach has its own strengths and limitations, combining two or more methods would provide additional modalities for cancer immunotherapy.

Herein, we developed a PEG-*b*-poly(L-alanine) hydrogel as a platform for co-delivery of a tumor vaccine and two immune checkpoint inhibitors. In contrast to other vaccine delivery carriers, such as PLGA and inorganic scaffolds [39, 66], polypeptide hydrogels have advantages including spontaneous assembly in aqueous solution without the use of crosslinking agents, during which drugs can be easily encapsulated without the loss of bioactivity. Moreover, the present polypeptide hydrogel can be easily administrated *in vivo* by injection using a syringe equipped with a 26-gauge needle (Figure S1C). Besides, the polypeptide hydrogel has acceptable biocompatibility *in vivo*. Commonly, only minimal acute inflammatory reactions in the subcutaneous tissue surrounding the injection site are found by H&E staining [55, 56, 67], and with degradation of the hydrogel, the inflammatory reaction would be eventually eliminated. In our previous study, we first reported a polypeptide hydrogel-based delivery of a tumor vaccine composed of tumor cell lysate and the TLR-3 agonist poly(I:C) [68]; we found that the tumor vaccine formulated in the hydrogel resulted in better anti-melanoma efficacy in mice compared with immunization by the free vaccine. Different from the previous tumor vaccine, GM-CSF was used here as an adjuvant that functions as a cytokine to help recruit and stimulate DCs. In addition, immune checkpoint inhibitors were used to supplement the hydrogel-based tumor vaccine to further increase antitumor efficacy. The results obtained in this study confirmed the benefit of combinatorial immunotherapy using a PEG-*b*-poly(L-alanine) hydrogel as the drug delivery system, which provides an alternative for vaccine delivery, immune checkpoint blockade and their combinations.

It is known that CTLA-4 and PD-1 proteins are upregulated in activated T cells, which is particularly notable in cancers. Clinical trials have shown that the combination of anti-CTLA-4 and anti-PD-1 therapy through intravenous injection can increase the objective response [5, 6]; however, their concurrent use results in more toxic effects. Local drug delivery strategies have emerged that show potential in reducing the toxicity of antibodies while maintaining or even improving their therapeutic efficacy [26, 69]. Since both pathways may affect T cells in tumor tissue, local delivery within or around tumor is rational and may increase the local concentration and decrease the systemic distribution. In this regard, fluorescence-labeled anti-PD-1 antibody was used to monitor the antibody release *in vivo*. The results shown in Figure S10 indicated that encapsulation of anti-PD-1 antibody in the hydrogel prolonged its

duration *in vivo*, and decreased the systemic distribution of the antibody. However, a portion of the antibody was released into organs including the lymph nodes, spleen, liver, lung, kidney and heart, which could explain why the systemic T-cell response was also amplified, despite the antibody being locally delivered. In addition, as shown in Figure S11, hydrogel-based co-delivery of the two inhibitors did not cause any toxic effects, while the injection of free antibodies increased the level of alanine aminotransferase and the leukocyte count, and decreased the platelet count and the hemoglobin content in blood, in comparison with blank controls, indicating possible hepatotoxicity and hematotoxicity. Local delivery of checkpoint inhibitors by the polypeptide hydrogel may be an effective approach to eliminate the toxicity associated with the administration of high-dose antibodies. Hydrogel-based combined blockage of both CTLA-4 and PD-1 was better than individual inhibition. And interestingly, CTLA-4 blockade conferred a better combinatorial anti-melanoma immune response over PD-1 inhibition at the same dosage, which was more evident in the spleen. This might be due to the inherent difference in the expression of surface PD-1 and CTLA-4 proteins on T cells and the percentage of PD-1<sup>+</sup> and CTLA-4<sup>+</sup> T cells in tumors or spleens.

Based on the results in this study, we can describe the immunotherapeutic mechanism as follows: first, the hydrogel-based spatiotemporal presentation of tumor cell lysates and GM-CSF recruited a large number of host DCs, which processed tumor antigens and became mature within the hydrogel with the assistance of GM-CSF. Then, mature DCs migrated to secondary lymphatic tissues and cross-presented antigenic peptides to T cells, thereby initiating antigen-specific T-cell priming. In the meantime, anti-PD-1 and anti-CTLA-4 therapy further enhanced the T-cell activation and the depletion of Tregs by inhibiting the immunosuppressive tumor microenvironment. Synergistically, a combination of the tumor vaccine and double checkpoint blockades in the hydrogel-based drug delivery system resulted in superior antitumor therapy.

## Conclusion

In summary, PEGylated polypeptide hydrogel was developed to co-deliver a tumor vaccine and two immune checkpoint inhibitors for combinatorial tumor immunotherapy. The hydrogel platform provided sustained release of tumor cell lysates, GM-CSF, and antibodies both *in vitro* and *in vivo*. Hydrogel vaccines efficiently recruited, activated endogenous DCs and elicited strong humoral and

cellular responses, including potent systemic CTL response, which clearly inhibited the tumor growth and reduced the tumor mass in combination with the dual checkpoints blockades. The hydrogel-based co-delivery system strikingly augmented the expansion of effector CD8<sup>+</sup> T cells within the spleens and tumors from immunized mice, while reducing the proportion of Tregs within the spleens and dLNs. Namely, the hydrogel-based combination immunotherapy can not only enhance the melanoma-specific CTL response but also attenuate the immunosuppressive tumorous environment. Collectively, the polypeptide hydrogel-based co-delivery system provided a promising treatment modality for cancers including, but not limited to melanoma and 4T-1 tumor.

## Supplementary Material

Supplementary methods, figures and table.  
<http://www.thno.org/v09p2299s1.pdf>

## Acknowledgements

We acknowledge the financial support from the National Natural Science Foundation of China (No. 31670977, 31870950, 51703246, 21604095), CAMS Innovation Fund for Medical Sciences (No. 2017-I2M-4-001, 2016-I2M-3-022, 2017-I2M-3-022), Key Projects of Advanced Manufacturing Technology for High Quality Veterinary Drugs (No. 17ZXGNC00080), the Non-profit Central Research Institute Fund of Chinese Academy of Medical Sciences (No. 2018RC350017), Tianjin Innovation and Promotion Plan Key Innovation Team of Immunoreactive Biomaterials, Specific Program for High-Tech Leader & Team of Tianjin Government, and Tianjin Natural Science Foundation (No. 17JCQNJC13800).

## Competing Interests

The authors have declared that no competing interest exists.

## References

- Hu Z, Ott PA, Wu CJ. Towards personalized, tumour-specific, therapeutic vaccines for cancer. *Nat Rev Immunol*. 2018; 18: 168-82.
- Schumacher TN, Schreiber RD. Neoantigens in cancer immunotherapy. *Science*. 2015; 348: 69-74.
- Sahin U, Türeci Ö. Personalized vaccines for cancer immunotherapy. *Science*. 2018; 359: 1355-60.
- Pardoll DM. The blockade of immune checkpoints in cancer immunotherapy. *Nat Rev Cancer*. 2012; 12: 252-64.
- Larkin J, Chiarion-Sileni V, Gonzalez R, Grob JJ, Cowey CL, Lao CD, et al. Combined nivolumab and ipilimumab or monotherapy in untreated melanoma. *N Engl J Med*. 2015; 373: 23-34.
- Wolchok JD, Kluger H, Callahan MK, Postow MA, Rizvi NA, Lesokhin AM, et al. Nivolumab plus ipilimumab in advanced melanoma. *N Engl J Med*. 2013; 369: 122-33.
- Davila ML, Riviere I, Wang X, Bartido S, Park J, Curran K, et al. Efficacy and toxicity management of 19-28z CAR T cell therapy in B cell acute lymphoblastic leukemia. *Sci Transl Med*. 2014; 6: 224ra25.
- Srivastava S, Riddell SR. Engineering CAR-T cells: Design concepts. *Trends Immunol*. 2015; 36: 494-502.
- Fan J, Shang D, Han B, Song J, Chen H, Yang JM. Adoptive cell transfer: Is it a promising immunotherapy for colorectal cancer?. *Theranostics*. 2018; 8: 5784-800.
- Ott PA, Hu Z, Keskin DB, Shukla SA, Sun J, Bozym DJ, et al. An immunogenic personal neantigen vaccine for patients with melanoma. *Nature*. 2017; 547: 217-21.
- Sahin U, Derhovanessian E, Miller M, Kloke B-P, Simon P, Löwer M, et al. Personalized RNA mutanome vaccines mobilize poly-specific therapeutic immunity against cancer. *Nature*. 2017; 547: 222-6.
- Kuai R, Ochyl LJ, Bahjat KS, Schwendeman A, Moon JJ. Designer vaccine nanodiscs for personalized cancer immunotherapy. *Nat Mater*. 2017; 16: 489-96.
- Pijpers F, Faint R, Saini N. Therapeutic cancer vaccines. *Nat Rev Drug Discov*. 2005; 4: 623.
- He X, Abrams SJ, Lovell JF. Peptide delivery systems for cancer vaccines. *Adv Therap*. 2018; 0: 1800060.
- Sette A, Fikes J. Epitope-based vaccines: an update on epitope identification, vaccine design and delivery. *Curr Opin Immunol*. 2003; 15: 461-70.
- Li AW, Sobral MC, Badrinath S, Choi Y, Graveline A, Stafford AG, et al. A facile approach to enhance antigen response for personalized cancer vaccination. *Nat Mater*. 2018; 17: 528-34.
- Singh A, Peppas NA. Hydrogels and scaffolds for immunomodulation. *Adv Mater*. 2014; 26: 6530-41.
- Talebian S, Foroughi J, Wade SJ, Vine KL, Dolatshahi-Pirouz A, Mehrli M, et al. Biopolymers for antitumor implantable drug delivery systems: Recent advances and future outlook. *Adv Mater*. 2018; 30: 1706665.
- Cheung AS, Mooney DJ. Engineered materials for cancer immunotherapy. *Nano Today*. 2015; 10: 511-31.
- Gosselin EA, Eppler HB, Bromberg JS, Jewell CM. Designing natural and synthetic immune tissues. *Nat Mater*. 2018; 17: 484-98.
- Reed SG, Orr MT, Fox CB. Key roles of adjuvants in modern vaccines. *Nat Med*. 2013; 19: 1597-608.
- Speiser DE, Ho P-C, Verdeil G. Regulatory circuits of T cell function in cancer. *Nat Rev Immunol*. 2016; 16: 599-611.
- Shao K, Singha S, Clemente-Casares X, Tsai S, Yang Y, Santamaria P. Nanoparticle-based immunotherapy for cancer. *ACS Nano*. 2015; 9: 16-30.
- Wang C, Ye Y, Hu Q, Bellotti A, Gu Z. Tailoring biomaterials for cancer immunotherapy: Emerging trends and future outlook. *Adv Mater*. 2017; 29: 1606036.
- Gao S, Yang D, Fang Y, Lin X, Jin X, Wang Q, et al. Engineering nanoparticles for targeted remodeling of the tumor microenvironment to improve cancer immunotherapy. *Theranostics*. 2019; 9: 126-51.
- Fan Q, Chen Z, Wang C, Liu Z. Toward biomaterials for enhancing immune checkpoint blockade therapy. *Adv Funct Mater*. 2018; 28: 1802540.
- Huang P, Wang X, Liang X, Yang J, Zhang C, Kong D, et al. Nano-, micro-, and macroscale drug delivery systems for cancer immunotherapy. *Acta Biomater*. 2019; 85: 1-26.
- Zhang C, Shi G, Zhang J, Song H, Niu J, Shi S, et al. Targeted antigen delivery to dendritic cell via functionalized alginate nanoparticles for cancer immunotherapy. *J Control Release*. 2017; 256: 170-81.
- Lee I-H, Kwon H-K, An S, Kim D, Kim S, Yu MK, et al. Imageable antigen-presenting gold nanoparticle vaccines for effective cancer immunotherapy in vivo. *Angew Chem Int Ed Engl*. 2012; 51: 8800-5.
- Rahimian S, Kleinovink JW, Fransen MF, Mezzanotte L, Gold H, Wisse P, et al. Near-infrared labeled, ovalbumin loaded polymeric nanoparticles based on a hydrophilic polyester as model vaccine: In vivo tracking and evaluation of antigen-specific CD8<sup>+</sup> T cell immune response. *Biomaterials*. 2015; 37: 469-77.
- Park J, Wrzesinski SH, Stern E, Look M, Criscione J, Ragheb R, et al. Combination delivery of TGF- $\beta$  inhibitor and IL-2 by nanoscale liposomal polymeric gels enhances tumour immunotherapy. *Nat Mater*. 2012; 11: 895-905.
- Rudra JS, Tian YF, Jung JP, Collier JH. A self-assembling peptide acting as an immune adjuvant. *Proc Natl Acad Sci U S A*. 2009; 107: 622-7.
- Li P, Zhou J, Huang P, Zhang C, Wang W, Li C, et al. Self-assembled PEG-*b*-PDPA-*b*-PGEM copolymer nanoparticles as protein antigen delivery vehicles to dendritic cells: Preparation, characterization and cellular uptake. *Regen Biomater*. 2017; 4: 11-20.
- Luo M, Wang H, Wang Z, Cai H, Lu Z, Li Y, et al. A STING-activating nanovaccine for cancer immunotherapy. *Nat Nanotechnol*. 2017; 12: 648-54.
- Rodell CB, Arlauckas SP, Cuccarese MF, Garriss CS, Li R, Ahmed MS, et al. TLR7/8-agonist-loaded nanoparticles promote the polarization of tumour-associated macrophages to enhance cancer immunotherapy. *Nat Biomed Eng*. 2018; 2: 578-88.
- Wang Y, Su L, Morin MD, Jones BT, Mifune Y, Shi H, et al. Adjuvant effect of the novel TLR1/TLR2 agonist Diprovocim synergizes with anti-PD-L1 to eliminate melanoma in mice. *Proc Natl Acad Sci U S A*. 2018; 115: E8698-E706.
- Kuai R, Sun X, Yuan W, Ochyl LJ, Xu Y, Hassani Najafabadi A, et al. Dual TLR agonist nanodiscs as a strong adjuvant system for vaccines and immunotherapy. *J Control Release*. 2018; 282: 131-9.
- Yang P, Song H, Qin Y, Huang P, Zhang C, Kong D, et al. Engineering dendritic cell-based vaccines and PD-1 blockade in self-assembled peptide nanofibrous hydrogel to amplify antitumor T-cell immunity. *Nano Lett*. 2018; 18: 4377-85.

39. Kim J, Li WA, Choi Y, Lewin SA, Verbeke CS, Dranoff G, et al. Injectable, spontaneously assembling, inorganic scaffolds modulate immune cells in vivo and increase vaccine efficacy. *Nat Biotechnol.* 2015; 33: 64-72.
40. Wang H, Luo Z, Wang Y, He T, Yang C, Ren C, et al. Enzyme-catalyzed formation of supramolecular hydrogels as promising vaccine adjuvants. *Adv Funct Mater.* 2016; 26: 1822-9.
41. Luo Z, Wu Q, Yang C, Wang H, He T, Wang Y, et al. A powerful CD8<sup>+</sup> T-cell stimulating D-tetra-peptide hydrogel as a very promising vaccine adjuvant. *Adv Mater.* 2017; 29: 1601776.
42. Wen Y, Waltman A, Han H, Collier JH. Switching the immunogenicity of peptide assemblies using surface properties. *ACS Nano.* 2016; 10: 9274-86.
43. Wang T, Wang D, Yu H, Feng B, Zhou F, Zhang H, et al. A cancer vaccine-mediated postoperative immunotherapy for recurrent and metastatic tumors. *Nat Commun.* 2018; 9: 1532.
44. Park CG, Hartl CA, Schmid D, Carmona EM, Kim H-J, Goldberg MS. Extended release of perioperative immunotherapy prevents tumor recurrence and eliminates metastases. *Sci Transl Med.* 2018; 10: eaar1916.
45. Ishihara J, Fukunaga K, Ishihara A, Larsson HM, Potin L, Hosseinchi P, et al. Matrix-binding checkpoint immunotherapies enhance antitumor efficacy and reduce adverse events. *Sci Transl Med.* 2017; 9: eaan0401.
46. Wang C, Wang J, Zhang X, Yu S, Wen D, Hu Q, et al. In situ formed reactive oxygen species-responsive scaffold with gemcitabine and checkpoint inhibitor for combination therapy. *Sci Transl Med.* 2018; 10: eaan3682.
47. Wang C, Sun W, Ye Y, Hu Q, Bomba HN, Gu Z. In situ activation of platelets with checkpoint inhibitors for post-surgical cancer immunotherapy. *Nat Biomed Eng.* 2017; 1: 0011.
48. Wang C, Ye Y, Hochu GM, Sadeghifar H, Gu Z. Enhanced cancer immunotherapy by microneedle patch-assisted delivery of anti-PD1 antibody. *Nano Lett.* 2016; 16: 2334-40.
49. Kostic M, Zivkovic N, Cvetanovic A, Stojanovic I. Granulocyte-macrophage colony-stimulating factor as a mediator of autoimmunity in multiple sclerosis. *J Neuroimmunol.* 2018; 323: 1-9.
50. Shi Y, Liu CH, Roberts AI, Das J, Xu G, Ren G, et al. Granulocyte-macrophage colony-stimulating factor (GM-CSF) and T-cell responses: what we do and don't know. *Cell Res.* 2006; 16: 126.
51. Song H, Yang G, Huang P, Kong D, Wang W. Self-assembled PEG-poly(L-valine) hydrogels as promising 3D cell culture scaffolds. *J Mater Chem B.* 2017; 5: 1724-33.
52. Zhang Y, Song H, Zhang H, Huang P, Liu J, Chu L, et al. Fine tuning the assembly and gel behaviors of PEGylated polypeptide conjugates by the copolymerization of L-alanine and  $\gamma$ -benzyl-L-glutamate N-carboxyanhydrides. *J Polym Sci A Polym Chem.* 2017; 55: 1512-23.
53. Li P, Shi G, Zhang X, Song H, Zhang C, Wang W, et al. Guanidinylated cationic nanoparticles as robust protein antigen delivery systems and adjuvants for promoting antigen-specific immune responses in vivo. *J Mater Chem B.* 2016; 4: 5608-20.
54. Li P, Song H, Zhang H, Yang P, Zhang C, Huang P, et al. Engineering biodegradable guanidyl-decorated PEG-PCL nanoparticles as robust exogenous activators of DCs and antigen cross-presentation. *Nanoscale.* 2017; 9: 13413-8.
55. Cheng Y, He C, Xiao C, Ding J, Cui H, Zhuang X, et al. Versatile biofunctionalization of polypeptide-based thermosensitive hydrogels via click chemistry. *Biomacromolecules.* 2013; 14: 468-75.
56. Yun EJ, Yon B, Joo MK, Jeong B. Cell therapy for skin wound using fibroblast encapsulated poly(ethylene glycol)-poly(L-alanine) thermogel. *Biomacromolecules.* 2012; 13: 1106-11.
57. Karavasilis C, Panteris E, Vizirianakis IS, Koutsopoulos S, Fatouros DG. Chemotherapeutic delivery from a self-assembling peptide nanofiber hydrogel for the management of glioblastoma. *Pharm Res.* 2018; 35: 166.
58. Selby MJ, Engelhardt JJ, Quigley M, Henning KA, Chen T, Srinivasan M, et al. Anti-CTLA-4 antibodies of IgG2a isotype enhance antitumor activity through reduction of intratumoral regulatory T cells. *Cancer Immunol Res.* 2013.
59. Simpson TR, Li F, Montalvo-Ortiz W, Sepulveda MA, Bergerhoff K, Arce F, et al. Fc-dependent depletion of tumor-infiltrating regulatory T cells co-defines the efficacy of anti-CTLA-4 therapy against melanoma. *J Exp Med.* 2013; 210: 1695-710.
60. Ingram JR, Blomberg OS, Rashidian M, Ali L, Garforth S, Fedorov E, et al. Anti-CTLA-4 therapy requires an Fc domain for efficacy. *Proc Natl Acad Sci U S A.* 2018; 115: 3912-7.
61. Sharma A, Subudhi SK, Blando J, Scutti J, Vence L, Wargo JA, et al. Anti-CTLA-4 immunotherapy does not deplete FOXP3<sup>+</sup> regulatory T cells (Tregs) in human cancers. *Clin Cancer Res.* 2018: clincanres.0762.2018.
62. Taube JM, Klein AP, Brahmer JR, Xu H, Pan X, Kim JH, et al. Association of PD-1, PD-1 ligands, and other features of the tumor immune microenvironment with response to anti-PD-1 therapy. *Clin Cancer Res.* 2014: clincanres.3271.2013.
63. Tumeq PC, Harview CL, Yearley JH, Shintaku IP, Taylor EJM, Robert L, et al. PD-1 blockade induces responses by inhibiting adaptive immune resistance. *Nature.* 2014; 515: 568.
64. Curran MA, Montalvo W, Yagita H, Allison JP. PD-1 and CTLA-4 combination blockade expands infiltrating T cells and reduces regulatory T and myeloid cells within B16 melanoma tumors. *Proc Natl Acad Sci U S A.* 2010; 107: 4275-80.
65. Fife BT, Pauken KE, Eagar TN, Obu T, Wu J, Tang Q, et al. Interactions between PD-1 and PD-L1 promote tolerance by blocking the TCR-induced stop signal. *Nat Immunol.* 2009; 10: 1185-92.
66. Ali OA, Huebsch N, Cao L, Dranoff G, Mooney DJ. Infection-mimicking materials to program dendritic cells in situ. *Nat Mater.* 2009; 8: 151-8.
67. Choi BG, Park MH, Cho S-H, Joo MK, Oh HJ, Kim EH, et al. In situ thermal gelling polypeptide for chondrocytes 3D culture. *Biomaterials.* 2010; 31: 9266-72.
68. Song H, Huang P, Niu J, Shi G, Zhang C, Kong D, et al. Injectable polypeptide hydrogel for dual-delivery of antigen and TLR3 agonist to modulate dendritic cells in vivo and enhance potent cytotoxic T-lymphocyte response against melanoma. *Biomaterials.* 2018; 159: 119-29.
69. Yu S, Wang C, Yu J, Wang J, Lu Y, Zhang Y, et al. Injectable bioresponsive gel depot for enhanced immune checkpoint blockade. *Adv Mater.* 2018; 30: 1801527.